Regional Studies in Marine Science 43 (2021) 101671

Contents lists available at ScienceDirect

Regional Studies in Marine Science

journal homepage: www.elsevier.com/locate/rsma

Reverse circulation in Bahía Santa Elena, North Pacific of Costa Rica

Alexandre Tisseaux-Navarro *, Juan Pablo Salazar-Ceciliano, Sergio Cambronero-Solano, J. Mauro Vargas-Hernández, Xiomara Marquez

Universidad Nacional, Department of Physics, Heredia, 86-3000, Costa Rica

ARTICLE INFO

Article history:
Received 28 April 2020
Received in revised form 3 February 2021
Accepted 4 February 2021
Available online 10 February 2021

Keywords:
Inverse estuary
Density profile
Residual current
Tropical Bay
Costa Rica

ABSTRACT

This work describes the water circulation of Bahía Santa Elena using velocity fields and hydrographic data obtained from a ship-mounted Acoustic Doppler Current Profiler and a vertical profiler Conductivity–Temperature–Depth sonde, during two campaigns in August and October of 2019. Data were taken in a cross-bay transect in the main channel of the Bahía Santa Elena during a complete tidal cycle. The hydrographic data obtained during the two sampling campaigns suggest a reverse estuarine circulation; tidally averaged values of density and water velocities revealed a dense outflow at the bottom layer in the bay. This is the first description of an inverse estuary circulation pattern in Costa Rica and the second in Central America. Understanding the hydrographic properties of the bay is crucial for undertaking future research projects on water quality and biological communities.

© 2021 Elsevier B.V. All rights reserved.

1. Introduction

A classic definition of an estuary is described as a semi-enclosed coastal system with communication with the ocean and in which sea water is diluted by water from the continent, however this does not occur in many estuaries in tropical regions (Valle-Levinson, 2010). Estuaries are classified as positive and negative estuaries depending on the circulation patterns. In a positive estuary, where the system's water is less dense than ocean water, the estuary water will tend to leave the system above the incoming ocean water flow (Valle-Levinson, 2010). An inverse estuary is an estuary in which freshwater input is less than the losses due to evaporation; such estuaries contain hypersaline water. In an inverse estuary, sea water enters the estuary to compensate for the losses due to evaporation, carrying salt which raises concentration (Descroix et al., 2020). This makes the inner water of the estuary denser than ocean water, and leaving the estuary below the ocean flow (Valle-Levinson, 2010).

One of the most important roles of tropical estuaries is that they usually are feeding grounds for juvenile species of fishes (Cowan et al., 2012; Sheaves et al., 2017). Estuaries are often acknowledged as nurseries for several species (Elliot and Dewailly, 1995). Only a few studies have described the circulation of coastal water bodies in Central America, so these types of estuaries remain not fully understood.

Bahía Santa Elena (BSE) is an estuary located (10° 55 '21.3 "N; 85° 48' 05.2" W) in the North Pacific coast of Costa Rica and connected to the Gulf of Santa Elena. The BSE has a NW–SE orientation and is connected to the ocean in the northern flank (Fig. 1). The BSE has an approximate area of 10 km ^{2}, 4 km long, and 2 km wide, with two minor freshwater inputs from riverlets. The tidal regime in this area has a semidiurnal predominant behavior, with an average range of 228 cm (Lizano, 2006).

This region is influenced by wind jets of 10 ms^{-1} on average in the boreal winter, generated due to the pressure difference between the Caribbean Sea and the Pacific Ocean of Central America. These winds interacts with the topography between the border of Nicaragua and Costa Rica (Clarke, 1988; Salazar-Ceciliano et al., 2018; Steenburgh et al., 1998), generating the Papagayo Wind Jet.

These wind jets influence the local circulation and generate upwelling in most of the North Pacific coast of Costa Rica, leading to the formation of cold and nutrient-rich waters in the surface layer, influencing the conditions of BSE (Ballestero and Coen, 2004; McCreary et al., 1989; Vargas, 2004). Superficial changes in the water induce a rapid increase in the phytoplankton biomass, which activates the food chain, and promotes the fisheries activities in this area (Vargas, 2004; Villalobos-Rojas et al., 2014). Seasonal variability of the wind may influence the circulation patterns inside the BSE and therefore is an important factor to be considered to classify the type of estuary in the BSE.

The aim of this research was to describe the water circulation of the BSE using velocity fields and hydrographic data from two preliminary surveying in August and October of 2019 as a first approach to classify the type of the estuary in the BSE. Considering that the BSE was declared a Marine Management Area in June 2018 to conserve and give sustainable use to marine resources in

Abbreviations: BSE, Bahía Santa Elena; CTD, Conductivity–Temperature–Depth; ADCP, Acoustic Doppler Current Profiler

* Corresponding author.
E-mail address: alexandre.tisseaux.navarro@una.cr (A. Tisseaux-Navarro).

https://doi.org/10.1016/j.rsma.2021.101671
2352-4855/© 2021 Elsevier B.V. All rights reserved.

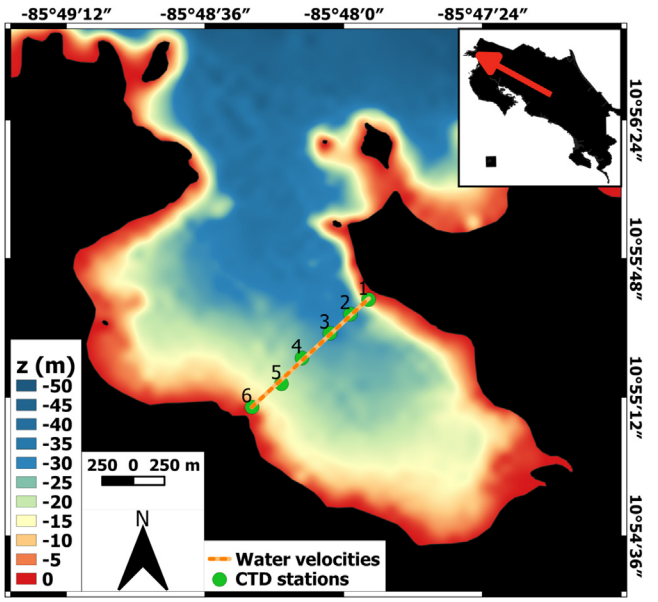

Fig. 1. Bathymetry map of Bahía Santa Elena with the transect for hydro acoustic current measurements (orange) and the CTD stations (1–6, green). Upper-right map indicates the geographic position of BSE in Costa Rica.. (For interpretation of the references to color in this figure legend, the reader is referred to the web version of this article.)

the area (MINAE, 2018), the findings from this work might also contribute to properly comply with a coastal management plan in the BSE.

2. Data and methods

In this section we describe the instruments and methodology used during the two surveys in August and October of 2019 to collect the observations of bathymetry, velocity fields and hydrographic data in the BSE.

The bathymetry survey was made with a Garmin echo sounder model EchoMap of 50 Hz and 200 Hz frequency; the data indicate that the deepest area is located in the northern flank with a maximum depth of 40 m (Fig. 1). We also observed that the eastern flank of the bay is deeper than the western flank.

We defined a 1200 m transect, transverse to the main channel of the BSE, to carry out the hydrographic measurements to describe residual temperature, residual current, residual density, residual chlorophyll concentration and the residual oxygen concentration (Fig. 1). Measurements were taken continuously during a complete semidiurnal tidal cycle (approximately 13 h) to guarantee the quality of the time series used for the data analysis.

Data sampling campaigns took place on August 20th, 2019, and October 2nd, 2019. On the first campaign, the maximum peak of the high tide (height of 2.65 m) was at 05:47 and the maximum of the next high tide (height of 2.47 m) was at 18:02, with the low tide (height of 0.25 m) at 11:50 (MIOCIOMAR, 2019). For the second campaign, on October 2nd of 2019, the first high tide was at 4:59 (height of 3.17 m), the low tide (height of −0.35 m) was at 11:11 and the following high tide at 17:26 (height of 2.91 m) (MIOCIOMAR, 2019).

The water velocities along the transect were measured with an Acoustic Doppler current meter (ADCP), model *M9* from *Sontek* mounted on a small vessel. The M9 ADCP is a nine-beam system with two sets of four profiling beams, 3- and 1-MHz transducers, and one vertical beam, with a maximum velocity profiling range of 40 m. The M9 has automatic adaptive sampling based on water depth and velocity to optimize the discharge measurement. Vertical profiles of temperature, chlorophyll concentration, dissolved oxygen and salinity were measured at six points along the transect (Fig. 1) using a Conductivity–Temperature–Depth sonde (CTD), model *SBE19-Plus* from *SeaBird*. This CTD has a sampling frequency of 4 Hz, the instrument was slowly casted at each point until reaching the sea bottom, only descending data was considered for this study.

A total of 11 transects were performed with the M9 in August and 10 in October. In both campaigns, CTD was cast 10 times in each of the six points, for a total of 66 profiles per campaign. Water flow measurements were processed with the help of the software Velocity Mapping Toolbox (VMT v4.09) (Parsons et al., 2013). Transects were interpolated with a horizontal and vertical grid node spacing of 25 m and 1 m, respectively. Based on signal quality, surface data of the first meter was blanked out of the analysis. Also, we estimated the flow in the perpendicular direction to the transect and that is named streamwise velocity from here on. Additionally, wind and precipitation data were obtained from a weather station model Vantage Pro2 from Davis, located on a coastal elevation 17 km east from BSE.

The residual current is defined as a flow after removing the tidal currents from the ADCP observations (Lwiza et al., 1991; Valle-Levinson and Bosley, 2003). Subtidal flows were determined from a least square fit of semidiurnal harmonics (Lunar M2) plus a subtidal contribution to the observations, through minimization of the difference between both sides of the following (Eq. (1)) relationship:

$$\mathbf{U = Uo + UM2cos(2\pi/TM2t - \varphi M2)} \quad (1)$$

where the 'U' indicates the current along the channel and 'Uo' refers to average or residual current. While UM2, TM2 and φM2 are the tidal velocity amplitude, period, and phase angle respectively, associated with the semidiurnal component (Lunar M2) of the tidal cycle. Additionally, the residual values (removing component M2) of temperature and salinity were also estimated using the same approach.

Additionally, we calculated Ke, the Kelvin number (Eq. (2)) for the study area, using the formula

$$\mathbf{Ke = B/Ri} \quad (2)$$

where B is the width of the basin, Ri is the internal Rossby radius and Ke is the Kelvin number (Garvine, 1995; Valle-Levinson, 2008). This number is estimated here to determine if BSE is classified as a narrow or wide system. A high Ke number represents a wide system (Ke $>$ 2), in which the system is influenced by Earth's rotation and flow is horizontally sheared (Valle-Levinson, 2010). In a narrow system, Earth's rotation does not determine whether the flow is vertically or horizontally sheared (Valle-Levinson, 2010).

3. Results

In this section, we introduce the hydrographic results collected with the CTD and the M9-ADCP during the two oceanographic campaigns in the BSE. The term "residual variable" in our study is associated with the result of removing the semi-diurnal tidal component during one full tidal cycle from the obtained observations.

The residual temperature in both days was higher at the surface level and lower with depth, by 1.2 °C in August and by 1.8 °C in October, showing a stratified column (Fig. 2A and B). Stations 1, 2, and 3 showed higher values compared to stations 4, 5, and 6 at the surface level (Fig. 2A and B). Consequently, observations in August showed warmer (approximately 1 °C) masses of water than in October.

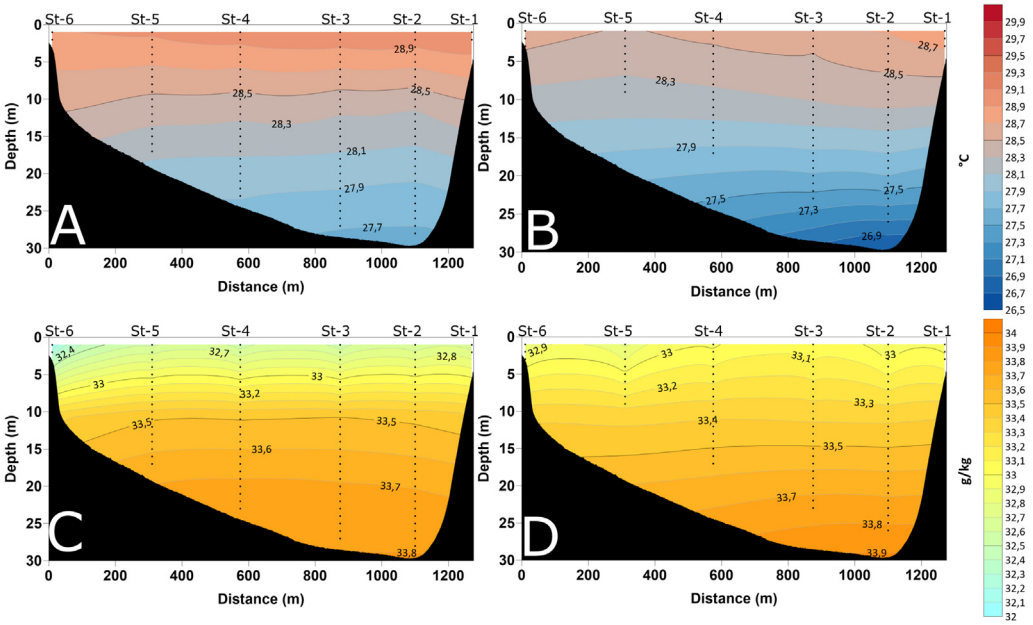

Fig. 2. Cross section of residual temperature (2A and 2 B)and residual salinity (2C and 2D), in the main channel of Bahía Santa Elena during one tidal cycle on August 20th 2019 (left, 2A, 2C) and October 2nd, 2019 (right, 2B, 2D). Black dots represent the CTD profiles, from station 6 at left to station 1 at right.

Residual salinity showed high values in the entire water column in both campaigns. For the October transect bottom water with the highest salinities is on the deepest section, in the eastern flank of the bay, with a maximum in salinity of around 33.9 g/kg. Surface water with the lowest salinity appeared in the first meters of the transect, with a minimum of around 32.8 g/kg. In August, maximum and minimum of salinity were found in the same area than those in October, corresponding to 33.8 g/kg and 32.1 g/kg.

The residual values of water flow in both campaigns showed horizontal and vertical gradients of the water velocities in the inner area of the bay (Fig. 3A and B). A shallow inflow of 5 to 12 cm s-1 was observed with less density (than the outflow) along the whole water column (Fig. 3C and D) from the southern part of the transect (left side on the maps in Fig. 3A and B) to the central section of the transect (stations 4, 5 and 6).

A weaker and more dense outflow ranging from 5 cm s^{-1} to 12 cm s^{-1} with a wedge shape from the sea bed to the surface was observed in the deepest section of the channel, extending from the middle of the transect to the northern flank (stations 1, 2 and 3, right side on the maps in Fig. 3A and B). This circulation pattern persisted during the entire measurement period, meaning outflow in the deeper section and inflow in the shallower section, however, we identified variations of the flow area and magnitude during the tidal cycle, with the latter varying between 10 and 15 cm s^{-1} and without exceeding the value of 30 cm s^{-1}.

Changes in water density in BSE were recorded during the tidal cycle. Taking station 2 as a reference point; higher density was observed across the water column during the beginning of the sampling with a decreasing trend over time (Fig. 4). This trend can be easily visualized by observing the deepening of the isopycnal of 1021.3 kg m^{-3} over-time in both campaigns, being more evident in October (Fig. 4).

The streamwise velocity also changed over time during both samplings at station 2 (Fig. 5). Water outflows were dominant at the beginning of the sampling and water inflows started to appear around midday, becoming stronger and prevailing until the end of both campaigns (Fig. 5). We observed that from midday there was an inflow (blue) at the surface and outflow (red) underneath, which is a typical inverse circulation based on the velocities and density values. To verify this circulation in BSE, we estimated a Rossby radius of 19 190 m and a basin width of 1200 m which resulted in a Kelvin number of 0.063 indicating a narrow estuary basin. Therefore, Earth's rotation is not likely to highly influence the flow in BSE.

Table 1
Meteorological conditions, recorded by the station located 17 km east of BSE, during each of the surveying days.

	August 20th	October 2nd
Average wind velocity (km/h)	7.59	9.10
Most frequent wind direction	North East	South
Total rain (mm)	9.80	1.30

Although it is normal to observe high precipitation values in climatologies from late August to late October throughout the North Pacific region, low precipitation rates and conditions of weak wind before and during both campaigns were observed. These anomalous dry conditions were particularly observed in October when normally is the rainiest month of the year based on climatologies (Table 1).

Based on precipitation records from the National Meteorological Institute of Costa Rica for the Santa Elena Area, the precipitation rate in August 2019 was 101.6 mm, showing 141.9 mm less than the climatological average for that month (IMN, 2019a). Similar behavior was observed in September 2019 (before the campaign on October 2nd), with a precipitation rate of 196.5 mm, showing 159.8 mm less than the climatological average (IMN, 2019b).

The concentration of oxygen and chlorophyll in station 2 varies with the tidal phase (Fig. 6), the values of both variables were higher during the flooding phase. We observed the highest values of oxygen concentration during the October survey, showing a layer of high concentration of oxygen as the flooding phase advances, reaching almost the entire water column at the end of the phase (Fig. 6C and D).

4. Discussion

This work describes the first attempt to characterize the circulation in Bahía Santa Elena during a complete tidal cycle. The

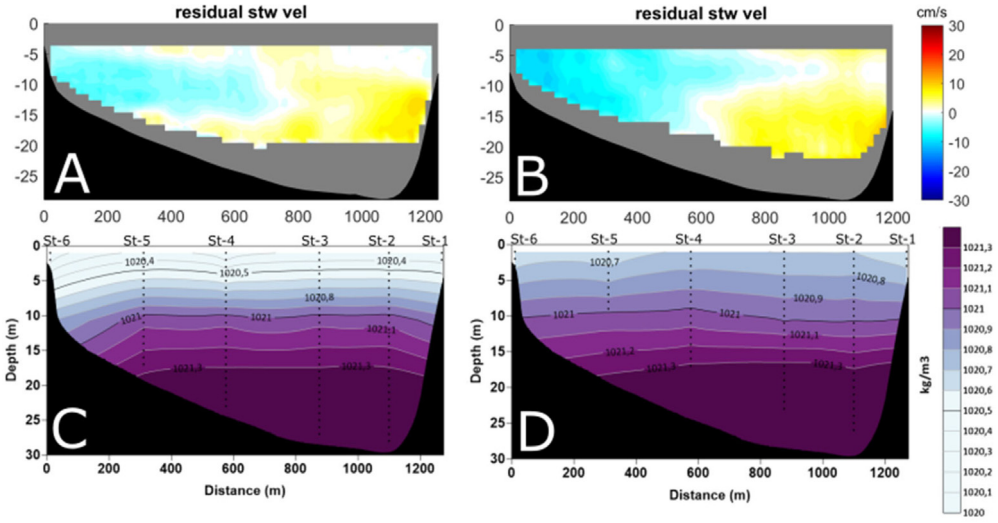

Fig. 3. Cross section of residual streamwise (stw) current (3 A and 3B) and residual density (3C and 3D) in the main channel of Bahía Santa Elena during one tidal cycle on August 20th, 2019 (left) and October 2nd, 2019 (right). In current figures positive values (red–yellow) represent outflow, and negative (blues) represent inflow. In density figures black dots represent the CTD profiles, from station 6 at left to station 1 at right.. (For interpretation of the references to color in this figure legend, the reader is referred to the web version of this article.)

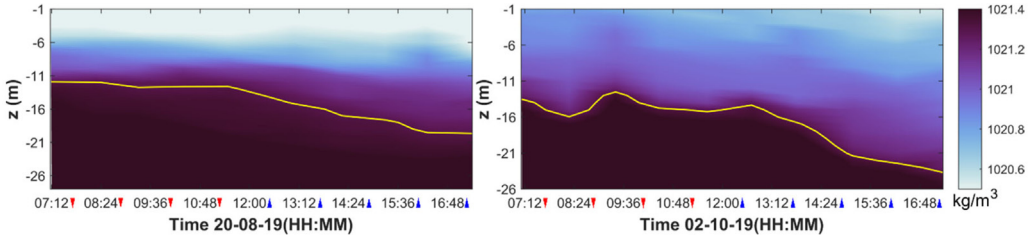

Fig. 4. Hovmöller diagram of density at station 2 of Bahía Santa Elena during one tidal cycle on August 20th, 2019 (left) and October 2nd, 2019 (right). Yellow line represents the isopycnal of 1021.3 kg/m^3. Arrows next to time values in the x axis represent the tidal phase at that moment, a red arrow for ebb phase and blue arrow for flood phase.. (For interpretation of the references to color in this figure legend, the reader is referred to the web version of this article.)

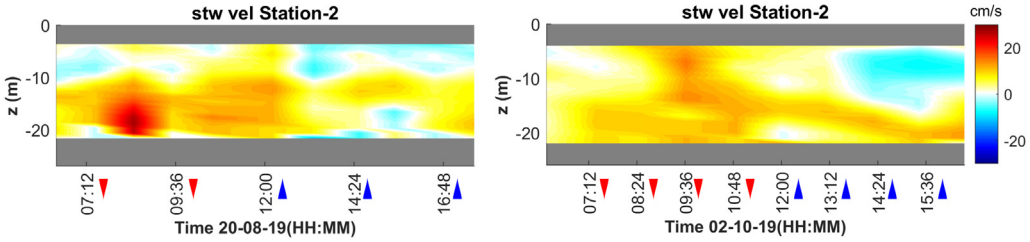

Fig. 5. Hovmöller diagram of streamwise velocity at station 2 of Bahía Santa Elena during one tidal cycle on August 20th, 2019 (left) and October 2nd, 2019 (right). Positive values (red and yellow) indicate water outflows and negative values (blues) indicates water inflows. Arrows next to time values in the x axis represent the tidal phase at that moment, a red arrow for ebb phase and blue arrow for flood phase.. (For interpretation of the references to color in this figure legend, the reader is referred to the web version of this article.)

hydrographic data obtained during the two sampling campaigns suggest a reverse estuarine circulation according to the definition of Valle-Levinson (2010); density and residual current values across the tidal cycle revealed a persisting dense outflow at the bottom of the bay. To our knowledge, this is the first description of an inverse estuary circulation pattern in Costa Rica and the second in Central America (Valle-Levinson and Bosley, 2003).

Our data suggest that there is an outflow near the surface at the northern side of the bay (main channel). Only evident in the October campaign, this could be because in October there was a larger gradient in temperature (by 0,2 degrees) between the northern and the southern side of the bay (see 28.7 °C isothermal, in Fig. 2B). We infer that this water comes from the surface of inner shallow areas of the bay (i.e. mangrove areas), where it is easily heated up, and comes out while staying at the surface, due to the fact that this water mass is less dense than the water underneath.

Vertical profiles of salinity and temperature show more homogeneous conditions in October (Figs. 2C, 2D, 3C and 3D) than in August. According to Geyer (2010), during spring tides, tidal mixing is maximal, and stratification should reach a minimum. This could explain the observed differences in the stratification patterns between both campaigns considering that the observations in October were taken near the spring tide with higher tidal ranges and tidal currents than in August.

Considering the low Kelvin number (Ke) value of 0.063 and based on the latitude and width of BSE which produces a large Rossby number, we conclude that the water flow in this bay is not importantly influenced by the earth rotation effect (Coriolis effect). Nevertheless, our results show a horizontal gradient in the

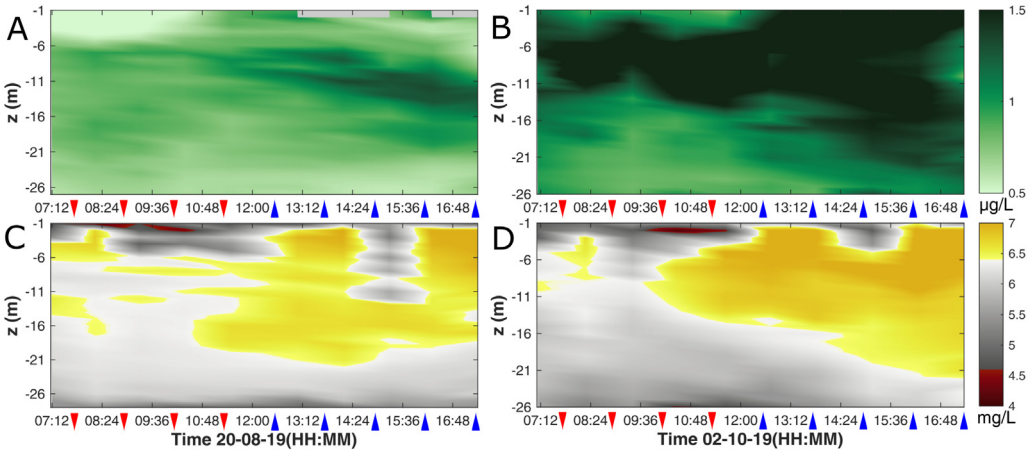

Fig. 6. Hovmöller diagram of chlorophyll (6A and 6B) and oxygen concentration (6C and 6D) at station 2 of Bahía Santa Elena during one tidal cycle on August 20th, 2019 (left, 6A and 6C) and October 2nd, 2019 (right, 6B and 6D). (For interpretation of the references to color in this figure legend, the reader is referred to the web version of this article.)

flow, which could be explained by high frictional conditions in the bay. Valle-Levinson (2008) explains that a horizontal sheared-flow can be found independently of the width of the basin, as long as high frictional conditions are present (Ek $>$ 1). Proper parametrization of the frictional forces needs to be done to better estimate the Ekman number in the BSE, this study is out of the scope of this paper and will be discussed deeply in a separate manuscript.

Our data show that density in the bay decreases during the flooding phase of the tidal cycle, meaning that the water density inside the bay is higher than the water coming from outside the bay. Figs. 4 and 5 show how the water column becomes less dense in both campaigns as the tide rises. Residual circulation, also known as the tidally averaged/subtidal circulation or estuarine exchange flow, governs this exchange between ocean and estuary and thus plays a large role in influencing these biological and biogeochemical processes (Giddings and MacCready, 2017). These are key to the fish nursery functioning of this bay, modulating the presence or absence of different species at different times of the tidal cycle.

During inverse exchange flow, the reversal manifests throughout depth with inflow at the surface and outflow at depth (Fig. 5). The inflow is trapped near the surface and the isohalines slope in the opposite direction compared to typical (positive estuary) exchange conditions. The momentum balance has similar dominant terms (with comparable magnitudes); however, we imply that the Coriolis and baroclinic pressure gradient terms have reversed vertical structure based on the obtained Ke number.

The conditions within the bay could be produced by a process of hyper salinization, which occurs in some estuarine systems with low freshwater input and high evaporation rates, causing water masses with higher density inside the system and therefore a reverse circulation behavior. The observations show high values of salinity, an indicator of low contribution of freshwater from rivers and low precipitation in the region during the sampling campaigns. According to the Meteorological Institute of Costa Rica (IMN, 2019a,b), there was a decrease in precipitation in the study area compared to previous years.

It has been observed in many estuarine systems that reverse circulation is not constant throughout the year, depending mainly on the weather conditions in the area (Nidzieko and Monismith, 2013; Valle-Levinson et al., 2001; Valle-Levinson and Bosley, 2003). Our data shows a snapshot of BSE conditions during a specific time, meaning that the variability of weather conditions could change the circulation patterns throughout the year. Lizano and Alfaro (2014) measured flow velocities across the water column in June 2012, and their observations agree with our findings regarding the stratification of the water flow. Therefore, we recommend replicating this experiment under different weather conditions; for example, during the dry season (December–March) of the Pacific slope, when the winds are stronger, and the surrounding area is influenced by the Papagayo upwelling (Clarke, 1988; Salazar-Ceciliano et al., 2018; Steenburgh et al., 1998). We also recommend replicating the experiment during high precipitation conditions to consider the influence of freshwater input from runoff.

Salinity values recorded in BSE are lower than those found in other reverse circulation systems where the values of salinity are usually as twice as high (Wolanski, 2013). The observations obtained here are similar to those found by Valle-Levinson and Bosley (2003) in the Gulf of Fonseca during the dry season, where the low supply of freshwater causes a reverse estuarine circulation. In the rainy season, the Gulf of Fonseca behaves like an estuary with typical circulation, it could be that the BSE also shows a typical circulation under conditions of a greater supply of freshwater than in our sampling campaigns. Furthermore, future research in this area might allow us to understand the variation of tropical estuaries under particular conditions like the influence of coastal upwelling, interannual variabilities such as El Niño Southern Oscillation and regional scale factors like the Papagayo upwelling system.

Our results show that tidal variation has an influences temperature, salinity, and chlorophyll concentration. We hypothesize that composition and abundance of planktonic communities are determined by this variation, as per Jendyk et al. (2014) indicated that in reverse circulation systems, salinity variation is the most determining factor in phytoplankton community composition.

Chlorophyll values indicate that conditions of the water masses entering to BSE increase the abundance of phytoplankton, promoting photosynthesis and thus increasing the concentration of oxygen within BSE, which could influence the abundance and diversity of fish populations in the BSE. This has been acknowledged by Hossain et al. (2017), Sánchez-Velasco et al. (2012), Silva et al. (2009), which concluded that in reverse estuarine circulation, as in normal estuarine circulation, the dynamics and composition of biological communities are influenced by variations in salinity, pH and oxygen concentration. Phytoplankton is the base of the trophic network in the ocean and produces much

of the oxygen necessary for the rest of the species in the system; a change in its diversity and abundance implies an effect on the rest of the living beings in the system. This explains how important it is to consider the tidal variations of water parameters for biological surveys, tourism and fisheries that take place in BSE.

5. Conclusions

Based on the data obtained in this study, we conclude that a reverse estuarine circulation occurs in BSE during periods of low precipitation and weak winds conditions. Therefore, we suggest that this particular circulation is not persistent throughout the year and that variability of weather conditions may have an important effect on the oceanographic dynamics inside the bay.

This study demonstrates the influence of the tidal cycle in the variation of water parameters in BSE. This is important as this bay was declared in 2008 as an "Important Site for Conservation" and since then the bay has been under constant evaluation of its ecosystemic services. Our results contribute to the state of knowledge for this area and improve baseline knowledge to design and conduct ecological assessments. We consider this as a contribution to better understand the ecological role of this bay as a nursery for commercially important species and as a refuge for migratory species such as humpback whales.

It is important to continue with hydrographic studies in the area, considering Costa Rican government's intentions to establish a harbor in this bay (Arias, 2016), this could represent a threat to the conservation of all species in the ecosystem. Also, Valle-Levinson (2010) explains that inverse estuaries are more prone to water quality problems than positive estuaries, due to their flushing being more sluggish than positive estuaries. Understanding the hydrographic properties of the bay may reduce the impact on water quality and biological communities.

CRediT authorship contribution statement

Alexandre Tisseaux-Navarro: Conceptualization, Software, Formal analysis, Investigation, Writing - original draft. **Juan Pablo Salazar-Ceciliano:** Conceptualization, Formal analysis, Writing - review & editing, Project administration. **Sergio Cambronero-Solano:** Methodology, Software, Investigation, Writing - original draft. **J. Mauro Vargas-Hernández:** Conceptualization, Investigation, Writing - review & editing, Project administration. **Xiomara Marquez:** Validation, Writing - review & editing.

Declaration of competing interest

The authors declare that they have no known competing financial interests or personal relationships that could have appeared to influence the work reported in this paper.

Acknowledgments

We would like to thank Braulio Juárez and Arnoldo Valle-Levinson for technical advisory. Also, to Captain Keylor Alfaro Lara for his collaboration in both surveys. To the reviewers for their suggestions to improve the document. Lastly to the 2019 Environmental Observatory grant program of Vicerrectoría de Investigación, Universidad Nacional.

Funding

The data collection and interpretation of this research was supported by the 2019 Environmental Observatory grant program of Vicerrectoría de Investigación, Universidad Nacional.

References

Arias, L., 2016. Costa Rica presents interoceanic canal project. Tico Times [WWW document]. URL https://ticotimes.net/2016/11/15/costa-rica-inter-oceanic-canal.

Ballestero, D., Coen, J.E., 2004. Generation and propagation of anticyclonic rings in the Gulf of Papagayo. Int. J. Remote Sens. http://dx.doi.org/10.1080/01431160310001642395.

Clarke, A.J., 1988. Inertial wind path and sea surface temperature patterns near the Gulf of Tehuantepec and Gulf of Papagayo. J. Geophys. Res. Ocean. http://dx.doi.org/10.1029/JC093iC12p15491.

Cowan, J.H., Yáñez-Arancibia, A., Sánchez-Gil, P., Deegan, L.A., 2012. Estuarine Nekton. In: Estuarine Ecology. http://dx.doi.org/10.1002/9781118412787.ch13.

Descroix, L., Sané, Y., Thior, M., Manga, S.P., Ba, B.D., Mingou, J., Mendy, V., Coly, S., Dièye, A., Badiane, A., Senghor, M.J., Diedhiou, A.B., Sow, D., Bouaita, Y., Soumaré, S., Diop, A., Faty, B., Sow, B.A., Machu, E., Montoroi, J.P., Andrieu, J., Vandervaere, J.P., 2020. Inverse estuaries in West Africa: Evidence of the rainfall recovery? Water (Switzerland) 12, http://dx.doi.org/10.3390/w12030647.

Elliot, M., Dewailly, F., 1995. 114719.pdf. J. Aquat. Ecol.

Garvine, R.W., 1995. A dynamical system for classifying buoyant coastal discharges. Cont. Shelf Res. 15, 1585–1596. http://dx.doi.org/10.1016/0278-4343(94)00065-U.

Geyer, W.R., 2010. Estuarine salinity structure and circulation. Contemp. Issues Estuar. Phys. 12–26. http://dx.doi.org/10.1017/CBO9780511676567.003.

Giddings, S.N., MacCready, P., 2017. Reverse Estuarine Circulation Due to Local and Remote Wind Forcing, Enhanced by the Presence of Along-Coast Estuaries. J. Geophys. Res.: Oceans 122 (12), 184–205. http://dx.doi.org/10.1002/2016JC012479.

Hossain, M.A., Hemraj, D.A., Ye, Q., Leterme, S.C., Qin, J.G., 2017. Diet overlap and resource partitioning among three forage fish species in Coorong, the largest inverse estuary in Australia. Environ. Biol. Fishes http://dx.doi.org/10.1007/s10641-017-0592-3.

IMN, 2019a. Boletín Meteorológico Mensual Agosto 2019. Inst. Meteorológico Nac. [WWW document]. URL https://www.imn.ac.cr/documents/10179/474355/AGOSTO.

IMN, 2019b. Boletín Meteorológico Mensual Setiembre 2019. Inst. Meteorológico Nac. [WWW document]. URL https://www.imn.ac.cr/documents/10179/474355/SETIEMBRE.

Jendyk, J., Hemraj, D.A., Brown, M.H., Ellis, A.V., Leterme, S.C., 2014. Environmental variability and phytoplankton dynamics in a South Australian inverse estuary. Cont. Shelf Res. 91, 134–144. http://dx.doi.org/10.1016/j.csr.2014.08.009.

Lizano, O., 2006. Algunas características de las mareas en la costa Pacífica y Caribe de Centroamérica. Cienc. Tecnol. Rev. Univ. Costa Rica 24, 51–64.

Lizano, O.G., Alfaro, E.J., 2014. Dinámica atmosférica y oceánica en algunos sitios del Área de Conservación Guanacaste (ACG). Costa Rica. Revista de Biologia Tropical 62, 17–31. http://dx.doi.org/10.15517/rbt.v62i4.20018.

Lwiza, K.M.M., Bowers, D.G., Simpson, J.H., 1991. Residual and tidal flow at a tidal mixing front in the North Sea. Cont. Shelf Res. 11, 1379–1395. http://dx.doi.org/10.1016/0278-4343(91)90041-4.

McCreary, J.P., Lee, H.S., Enfield, D.B., 1989. The response of the coastal ocean to strong offshore winds: With application to circulations in the Gulfs of Tehuantepec and Papagayo. J. Mar. Res. http://dx.doi.org/10.1357/002224089785076343.

MINAE, 2018. Creación del Área Marina de Manejo Bahía Santa Elena. [WWW document]. URL http://www.pgrweb.go.cr/scij/Busqueda/Normativa/Normas/nrm_texto_completo.aspx?param1=NRTC&nValor1=1&nValor2=87256&nValor3=113608&strTipM=TC.

MIOCIOMAR, 2019. Predicciones de mareas. [WWW document]. URL http://www.miocimar.ucr.ac.cr/mareas/38/.

Nidzieko, N.J., Monismith, S.G., 2013. Contrasting seasonal and fortnightly variations in the circulation of a seasonally inverse estuary, Elkhorn Slough, California. Estuaries Coasts http://dx.doi.org/10.1007/s12237-012-9548-1.

Parsons, D.R., Jackson, P.R., Czuba, J.A., Engel, F.L., Rhoads, B.L., Oberg, K.A., Best, J.L., Mueller, D.S., Johnson, K.K., Riley, J.D., 2013. Velocity Mapping Toolbox (VMT): A processing and visualization suite for moving-vessel ADCP measurements. Earth Surf. Process. Landf. 38, 1244–1260. http://dx.doi.org/10.1002/esp.3367.

Salazar-Ceciliano, J., Trasviña Castro, A., González-Rodríguez, E., 2018. Coastal currents in the Eastern Gulf of Tehuantepec from coastal altimetry. Adv. Sp. Res. 62, 866–873. http://dx.doi.org/10.1016/j.asr.2018.05.033.

Sánchez-Velasco, L., Lavín, M.F., Jiménez-Rosenberg, S.P.A., Montes, J.M., Turk-Boyer, P.J., 2012. Larval fish habitats and hydrography in the Biosphere Reserve of the Upper Gulf of California (June 2008). Cont. Shelf Res. 33, 88–99. http://dx.doi.org/10.1016/j.csr.2011.11.009.

Sheaves, M., Baker, R., Abrantes, K.G., Connolly, R.M., 2017. Fish biomass in tropical estuaries: Substantial variation in food web structure, sources of nutrition and ecosystem-supporting processes. Estuaries Coasts http://dx.doi.org/10.1007/s12237-016-0159-0.

Silva, A.M.A., Barbosa, J.E.L., Medeiros, P.R., Rocha, R.M., Lucena-Filho, M.A., Silva, D.F.S., 2009. Zooplankton (Cladocera and Rotifera) variations along a horizontal salinity gradient and during two seasons (dry and rainy) in a tropical inverse estuary (Northeast Brazil). Pan-American J. Aquatic Sci. 4 (2), 226–238.

Steenburgh, W.J., Schultz, D.M., Colle, B.A., 1998. The structure and evolution of gap outflow over the Gulf of Tehuantepec, Mexico. Mon. Weather Rev. http://dx.doi.org/10.1175/1520-0493(1998)126<2673:TSAEOG>2.0.CO;2.

Valle-Levinson, A., 2008. Density-driven exchange flow in terms of the Kelvin and Ekman numbers. J. Geophys. Res. Ocean. 113, http://dx.doi.org/10.1029/2007JC004144.

Valle-Levinson, A., 2010. Definition and classification of estuaries. In: Contemporary Issues in Estuarine Physics. http://dx.doi.org/10.1017/CBO9780511676567.002.

Valle-Levinson, A., Bosley, K.T., 2003. Reversing circulation patterns in a tropical estuary. J. Geophys. Res. C Oceans 108, 1–13. http://dx.doi.org/10.1029/2003jc001786.

Valle-Levinson, A., Delgado, J.A., Atkinson, L.P., 2001. Reversing water exchange patterns at the entrance to a semiarid coastal lagoon. Estuar. Coast. Shelf Sci. 53, 825–838. http://dx.doi.org/10.1006/ecss.2000.0813.

Vargas, J.M., 2004. Interacción océano-atmósfera: surgencia y generación de anillos en la región de Papagayo. Revista Geográfica de América Central 1 (40), 133–144.

Villalobos-Rojas, F., Herrera-Correal, J., Garita-Alvarado, C., Clarke, T., Beita-Jiménez, A., 2014. Actividades pesqueras dependientes de la ictiofauna en el Pacífico Norte de Costa Rica. Rev. Biol. Trop. http://dx.doi.org/10.15517/rbt.v62i4.20038.

Wolanski, E., 2013. Estuaries of Australia in 2050 and Beyond. Springer.